THE JOURNAL OF PHYSICAL CHEMISTRY B

Article

pubs.acs.org/JPCB

Spectroscopic Characterization and Modeling of Quadrupolar Charge-Transfer Dyes with Bulky Substituents

Cristina Sissa,[†] Francesca Terenziani,[†] Anna Painelli,*[,†] Raja Bhaskar Kanth Siram,[‡] and Satish Patil[‡]

[†]Dipartimento di Chimica GIAF and INSTM-UdR Parma, Università di Parma, Parco Area delle Scienze 17/a, 43124 Parma, Italy

[‡]Solid State and Structural Chemistry Unit, Indian Institute of Science, Bangalore 560012, India

Supporting Information

ABSTRACT: Joint experimental and theoretical work is presented on two quadrupolar D-π-A-π-D chromophores characterized by the same bulky donor (D) group and two different central cores. The first chromophore, a newly synthesized species with a malononitrile-based acceptor (A) group, has a V-shaped structure that makes its absorption spectrum very broad, covering most of the visible region. The second chromophore has a squaraine-based core and therefore a linear structure, as also evinced from its absorption spectra. Both chromophores show an anomalous red shift of the absorption band upon increasing solvent polarity, a feature that is ascribed to the large, bulky structure of the molecules. For these molecules, the basic description of polar solvation in terms of a uniform reaction field fails. Indeed, a simple extension of the model to account for two independent reaction fields associated with the two molecular arms quantitatively reproduces the observed linear absorption and fluorescence as well as fluorescence anisotropy spectra, fully rationalizing their nontrivial dependence on solvent polarity. The model derived from the analysis of linear spectra is adopted to predict nonlinear spectra and specifically hyper-Rayleigh scattering and two-photon absorption spectra. In polar solvents, the V-shaped chromophore is predicted to have a large HRS response in a wide spectral region (approximately 600−1300 nm). Anomalously large and largely solvent-dependent HRS responses for the linear chromophores are ascribed to symmetry lowering induced by polar solvation and amplified in this bulky system by the presence of two reaction fields.

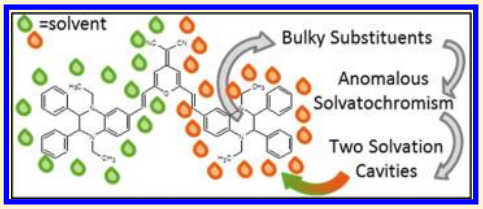

1. INTRODUCTION

Charge-transfer chromophores represent a wide class of π-conjugated molecules where the presence of electron-donor (D) and -acceptor (A) groups ensures the occurrence of low-energy excited states with large transition dipole moments. Polar (D-π-A) chromophores are good polarity sensors[1−5] and may show large nonlinear optical response,[6−12] and some of them behave as molecular rectifiers.[13−17] Quadrupolar (D-π-A-π-D or A-π-D-π-A) dyes were specifically developed as two-photon absorbers,[18−22] and some of them proved particularly interesting for two-photon-induced photodynamic therapy.[22−24] The important fluorescence solvatochromism shown by some quadrupolar dyes makes them also interesting for polarity- and voltage-sensing applications,[25,26] while quadrupolar structures were recently considered as light-harvesting species in solar cells.[27]

An extensive joint experimental and theoretical study[28] led to the definition of three different classes of quadrupolar chromophores, according to their spectroscopic behavior. Class I dyes show nonsolvatochromic absorption, as expected for nonpolar dyes, but due to the occurrence of symmetry breaking in the first excited state, they show a strongly solvatochromic fluorescence. Class II chromophores do not undergo symmetry breaking, and their spectra are marginally affected by solvent polarity. Finally, class III dyes undergo symmetry breaking in the ground state and show an important inverse solvatochromism of the absorption band, while their fluorescence spectrum is marginally affected by solvent polarity. Several examples are known for class I dyes,[19,28−30] while class II dyes are comprised of the very interesting family of squaraine-based dyes.[23−25,28] Class III behavior has been only recently recognized in cyanine dyes undergoing symmetry breaking in polar solvents.[31] The three-state model that describes the spectroscopic behavior of quadrupolar chromophores has been recently extended to account for bent quadrupolar structures.[32]

In this paper, we present an extensive study of optical spectra of the two quadrupolar dyes shown in Scheme 1. The two dyes include a newly synthesized malononitrile derivative, **1**, and a squaraine-based dye, **2**.[33] In both cases, the D groups attached to the central acceptor consist of the bulky 1,4-diethyl-2,3-diphenyl-1,2,3,4-tetrahydroquinoxaline-6-carbaldehyde group. Absorption spectra of both dyes show an anomalous solvatochromism that cannot be reconciled with the standard models for quadrupolar dyes,[28,32] calling for the definition of a new model. Specifically, we will extend the standard model for quadrupolar dyes to account for two solvent cavities, in line with the presence of bulky groups. The model quantitatively describes optical spectra of the two dyes and suggests large and nontrivial solvent effects in their nonlinear optical responses.

Received: January 17, 2012
Revised: April 1, 2012
Published: April 2, 2012

dx.doi.org/10.1021/jp3005508 | J. Phys. Chem. B 2012, 116, 4959−4966

Scheme 1. Molecular Structures of the Investigated Compounds

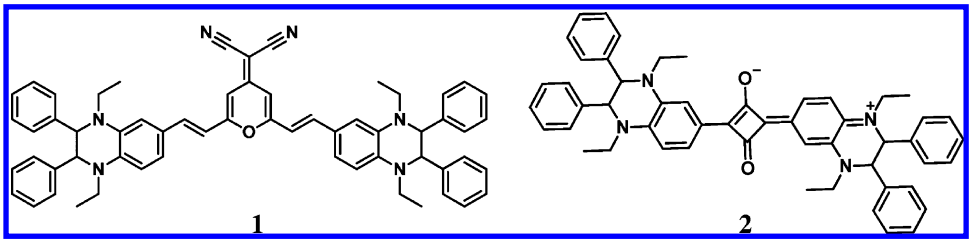

Scheme 2. Synthesis of D-π-A-π-D Chromophore 1

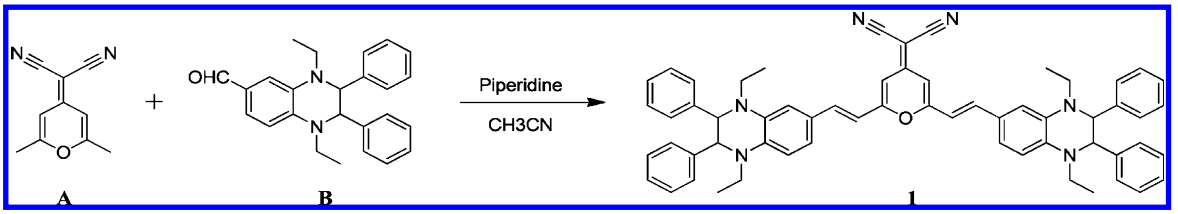

2. EXPERIMENTAL PROCEDURES

Materials. Analytical-grade solvents were used in the synthetic procedures. The squaraine dye **2** shown in Scheme 1 and 2,3-diphenylquinoxaline, 1,4-diethyl-2,3-diphenyl-1,2,3,4-tetrahydroquinoxaline, and 2-(2,6-dimethyl-4*H*-pyran-4-ylidene)malononitrile were synthesized according to literature procedures.[34−36] ^{1}H NMR and ^{13}C NMR spectra were recorded on a Bruker 400 MHz spectrophotometer in $CDCl_3$. Chemical shifts are given in parts per million (ppm) and coupling constants (J) in Hertz.

Synthesis of 2-(2,6-Bis((*E*)-2-(1,4-diethyl-2,3-diphenyl-1,2,3,4-tetrahydroquinoxalin-6-yl)vinyl)-4*H*-pyran-4-ylidene)malononitrile (1). Piperidine (0.2 mL) was added under an argon atmosphere to a mixture of 2-(2,6-dimethyl-4*H*-pyran-4-ylidene)malononitrile (0.162 g, 0.94 mmol) and 1,4-diethyl-2,3-diphenyl-1,2,3,4-tetrahydroquinoxaline-6-carbaldehyde (0.7 g, 1.88 mmol) in dry acetonitrile. The reaction mixture was refluxed for about 24 h. It was concentrated, and the compound was purified by using column chromatography. The total yield was 0.54 g (65%). NMR (400 MHz, $CDCl_3$): δ 7.47 (d, J = 16 Hz, 2H), 7.12 (m, 4H), 7.03 (t, J = 8 Hz, 10H), 6.96 (br, 2H), 6.71 (m, 10H), 6.55 (s, 2H), 6.52 (d, J = 16 Hz, 2H), 4.55 (d, J = 4 Hz, 4H), 3.44 (m, 4H), 3.12 (m,4H), 1.03 (t, J = 8 Hz, 6H), 1.00 (t, J = 8 Hz, 6H). ^{13}C NMR (100 MHz, $CDCl_3$): δ 139.09, 138.68, 138.35, 138.23, 135.24, 129.39, 129.28, 127.57, 124.04, 121.03, 116.53, 113.55, 113.04, 110.76, 109.94, 105.29, 65.68, 64.20, 43.71, 42.60, 11.16, 10.42. FTIR (KBr): 2925, 2854, 2202, 1634, 1518, 1489, 1412, 1351, 1261, 1170 cm^{-1}. HRMS [found: m/z 877.4601 $[M + H]^+$; calcd for $C_{60}H_{56}N_6O$ $[M + H]^+$: 877.4594].

Spectroscopic Measurements. Solvents used for spectroscopic measurements: cyclohexane (Sigma-Aldrich, HPLC); toluene (Sigma-Aldrich, ≥99.9%); 2-MeTHF (Sigma-Aldrich, anhydrous, ≥99.5%); dichloromethane (Sigma-Aldrich, ≥99.9%); dimethylsulfoxide (Riedel-de Haën, 99.5%); and glycerol (Sigma-Aldrich, anhydrous, ≥99.0%). 2-MeTHF was used after overnight storage on molecular sieves (0.3 nm); other solvents were used as received.

Absorption spectra were collected on a Lambda 650 UV/vis Perkin-Elmer spectrophotometer. The Beer−Lambert law was verified in measurements of the molar extinction coefficients. Emission spectra were recorded on a Fluoromax-3 Horiba Jobin-Yvon spectrofluorometer. To minimize self-absorption, emission and excitation spectra were measured on solutions with a concentration of ∼10^{-6} M. Fluorscein in NaOH 0.1 M was used as the standard for fluorescence quantum yield measurements (ϕ = 90%).

Fluorescence excitation anisotropy spectra were collected on a Fluoromax-3 Horiba Jobin-Yvon spectrofluorometer equipped with excitation and emission Glan-Thompson automatic polarizers for anisotropy measurements (single-channel L-format). Fluorescence anisotropy is defined as

$$r = \frac{I_{\parallel} - I_{\perp}}{I_{\parallel} + 2I_{\perp}} \quad (1)$$

where $I_{\parallel}$ is the emission intensity measured when the excitation and emission polarizers are parallel, while $I_{\perp}$ is the emission intensity when the two polarizers are mutually perpendicular. Further information on fluorescence anisotropy measurements can be found in ref 37.

3. RESULTS

Knoevenagel condensation of 2-(2,6-dimethyl-4*H*-pyran-4-ylidene)malononitrile (**A**) with 1,4-diethyl-2,3-diphenyl-1,2,3,4-tetrahydroquinoxaline-6-carbaldehyde (**B**) in the presence of piperidine gives the D-A-D chromophore **1** (see Scheme 2). Chromophore **2** was synthesized by the earlier reported procedure.[36] All of these dyes were characterized by ^{1}H NMR, ^{13}C NMR, HRMS, and IR spectroscopy.

Absorption and emission spectra of **1** and **2** collected in solvents of different polarity are shown in Figure 1. The main spectroscopic data are summarized in Table 1. The broad absorption spectrum of **1** spans a large portion of the visible spectral region, from red−orange to UV, with a very intense peak (hereafter, the main peak) in the green region and a weaker peak (the secondary peak) in the blue−violet region. Both peaks are weakly solvatochromic (shifts of 1230 and 780 cm^{-1} from cyclohexane to dichloromethane for the main and the secondary peaks, respectively), an unusual result for quadrupolar chromophores.[28] Fluorescence spectra show a more important solvatochromism, as expected for largely neutral (class I) quadrupolar dyes with a broken-symmetry fluorescent state;[28] the emission band shifts to the red by about 3600 cm^{-1} from cyclohexane to dichloromethane, and the Stokes shift increases with solvent polarity up to ∼5000 cm^{-1} in

dx.doi.org/10.1021/jp3005508 | J. Phys. Chem. B 2012, 116, 4959−4966

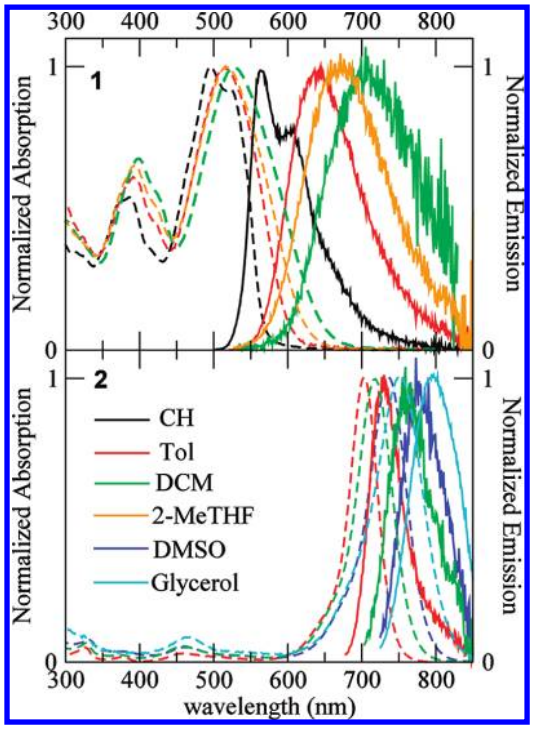

Figure 1. Experimental absorption and emission spectra of **1** (top panel) and **2** (bottom panel) in solvents of different polarity.

dichloromethane. Absorption and emission spectra collected in cyclohexane show a resolved vibronic structure, but the spectra broaden in polar solvents. The spectral behavior of **2** is qualitatively different; absorption and emission bands are very narrow, and the solvatochromic behavior is less pronounced than that for **1** (shifts of ~900 and ~1100 cm^{-1} for the absorption and the emission bands, respectively, from toluene to glycerol). The observed Stokes shifts are small in all of the solvents. The fluorescence quantum yield of **1** and **2** is high in nonpolar solvents and drastically decreases in solvents of medium and high polarity. The decrease of the fluorescence quantum yield in polar solvents can be ascribed to several reasons. First, emission is red-shifted in polar solvents, so that the probability of the process, scaling with the third power of the transition frequency, decreases. Moreover, the efficiency of the emission process is strongly environment-dependent and hardly predictable because several nonradiative processes, including collisional events, internal conformational conversions, and so forth, compete with radiative emission. In any case, the very weak fluorescence observed in polar solvents will be compared below with the emission calculated from a thermalized excited state. This is in line with the thermalization process, driven by solvent relaxation (typically in the picosecond regime[38]), being faster than fluorescence lifetimes (typically in the nanosecond regime).[39]

To gain more insight into the nature of the excited states, we measured fluorescence anisotropy spectra, as reported in Figure 2, at 77 K in 2-MeTHF for **1** and at room temperature in glycerol for **2**. Glycerol, being highly viscous at ambient temperature, is a good solvent for fluorescence anisotropy measurements.[40] Unfortunately, the fluorescence signal of **1** in glycerol is too weak; therefore, anisotropy data for **1** were obtained in glassy 2-MeTHF matrixes. The fluorescence anisotropy spectrum of **2** is flat within the excitation band and very close to the limiting r = 0.4 value, as expected for linear molecules,[39] whose absorption and fluorescence transition dipole moments are aligned along the main molecular axis. On the opposite, the anisotropy of **1** smoothly decreases from ~0.37 to ~0.3 within the main excitation band at 500 nm, then showing a sharp decrease in correspondence of the secondary band at about 400 nm.

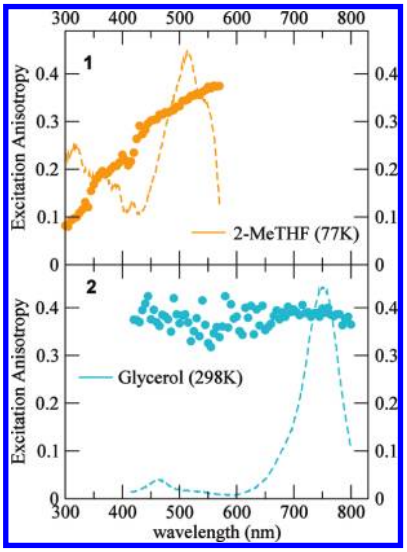

Figure 2. Experimental fluorescence excitation anisotropy (dots). (Top panel) **1** in glassy 2-MeTHF at T = 77 K. (Bottom panel) **2** in glycerol at room temperature. Dashed lines in both panels show fluorescence excitation spectra collected under the same experimental conditions as those adopted for anisotropy measurements.

Table 1. Experimental Spectroscopic Data Relevant to Molecules 1 and 2 in Solvents of Different Polarity

	solvent	λ_{abs}(nm)[a]	λ_{em}(nm)[a]	Stokes shift (cm^{-1})	ε (mol^{-1} cm^{-1})[b]	ϕ (%)[c]
1	cyclohexane	495/387	563	2440		22
	toluene	515/391	642	3841	51400	38
	2-MeTHF	518/395	672	4424		
	dichloromethane	527/399	705	4791		
2	toluene	703	730	516	187000	43
	dichloromethane	718	761	787		4
	dimethylsulfoxide	736	780	766		
	glycerol	750	796	771		

[a]Absorption and emission wavelengths refer to band maxima. For absorption of **1**, the two wavelengths refer to the main/secondary peak. [b]Molar extinction coefficient. [c]Fluorescence quantum yields (in polar solvents, the quantum yield is too small, <1%, to be reliably estimated).

dx.doi.org/10.1021/jp3005508 | J. Phys. Chem. B 2012, 116, 4959−4966

4. ESSENTIAL-STATE MODELING

Quadrupolar chromophores, with D-π-A-π-D or A-π-D-π-A structure, have been classified in three different families according to their spectroscopic behavior.[28] However, neither **1** nor **2**, both having the classical A-π-D-π-A structure of quadrupolar dyes, conform to the standard picture. Both dyes in fact show a normally solvatochromic absorption band (i.e., the band moves to the red in polar solvents), while in the standard model, only class III dyes show a solvatochromic absorption, but in that case, an *inverse* solvatochromism is expected (i.e., the absorption band should move to the blue in polar solvents). For molecule **1**, some solvatochromism can be ascribed to its bent structure, but as shown in Figures S1 and S2 in the Supporting Information, to quantitatively recover the observed solvatochromism, one should impose an unphysically small angle between the two molecular arms (about 90°) that would also lead to an exceedingly large intensity of the secondary absorption band. On the other hand, dye **2** has a linear structure, and the standard model fails badly in reproducing its spectra (cf Figure S3 in the Supporting Information). Experimental data for **1** and **2** then call for some new mechanism.

The solvation model is a delicate issue in the description of quadrupolar chromophores. Specifically, in the standard model developed in ref 28 and recently extended to cyanine dyes,[31] the solute, located in a cavity inside of the solvent, feels a uniform electric field (the reaction field) generated by the reorientation of the solvent molecules around the solute. This highly approximate scheme yields to reasonably accurate results in most cases but is expected to fail for large molecules with bulky and flexible substituents, like the ones discussed in this work. Describing the solvatochromism of quadrupolar dyes accounting for a single reaction field implies in fact the assumption of coherent behavior between the two molecular arms, or, in other terms, it implies assuming that the excitation hops too fast between the two molecular harms to allow the solvent to relax. In the case of bulky groups, however, this implicit assumption of coherence may break down; due to local relaxation pathways, the excitation can reside on each arm long enough to allow the solvent to independently relax around each molecular arm, so that two reaction fields, relevant to the two arms, must be introduced. In a different perspective, two independent reaction fields can account for a nonuniform reaction field in the cavity, as expected for extended molecules. Extending the standard model to account for two different reaction fields leads to a new model that, as discussed below, quantitatively accounts for the spectral behavior of **1** and **2**.

As for the electronic structure, both **1** and **2** can be described in terms of three basis states,[28] corresponding to the three main resonance structures, a neutral state, $|N\rangle$ = DAD, and two zwitterionic states $|Z_1\rangle = DA^-D^+$ and $|Z_2\rangle = D^+A^-D$. The two degenerate zwitterionic states are separated by an energy gap 2η from the neutral state. A nonvanishing matrix element, $-(2)^{1/2}t$, mixes $|N\rangle$ with $|Z_1\rangle$ and $|Z_2\rangle$. The diagonalization of the electronic problem is conveniently done on a symmetrized basis with $|Z_\pm\rangle$ corresponding to the in-phase and out-of-phase combination of $|Z_1\rangle$ and $|Z_2\rangle$. The linear combination of the two symmetric basis states, $|N\rangle$ and $|Z_+\rangle$, leads to two symmetric eigenstates, $|g\rangle$ and $|e\rangle$, while the antisymmetric state stays unmixed, $|c\rangle = |Z_-\rangle$. For linear centrosymmetric molecules, the lowest-energy $|g\rangle \rightarrow |c\rangle$ transition is one-photon-allowed, while the $|g\rangle \rightarrow |e\rangle$ transition is two-photon-allowed. This simple scheme must be slightly modified in bent molecules where the reduced symmetry makes the two transitions allowed both in linear absorption (OPA) and two-photon absorption (TPA) spectra.[32] These simple considerations rationalize the appearance of the secondary bands in linear absorption spectra of **1**. However, a thorough analysis of optical spectra accounting for band shapes and solvatochromism requires a more detailed modeling, including vibrational and solvation degrees of freedom. We introduce two effective vibrational coordinates, q_1 and q_2, with the same frequency ω_ν and relaxation energy ε_ν, to describe the relaxation of the molecular geometry upon excitation on each molecular arm. The molecular Hamiltonian reads[28]

$$H_M = 2\eta(\hat{\rho}_1 + \hat{\rho}_2) - \sqrt{2}\,t\hat{\sigma} - \sqrt{2\varepsilon_\nu}\,\omega_\nu(\hat{q}_1\hat{\rho}_1 + \hat{q}_2\hat{\rho}_2) + \frac{1}{2}(\omega_\nu^2\hat{q}_1^2 + \omega_\nu^2\hat{q}_2^2 + \hat{p}_1^2 + \hat{p}_2^2) \quad (2)$$

where $\hat{\rho}_i = |Z_i\rangle\langle Z_i|$ and $\hat{\sigma} = \sum_{i=1}^{2} |N\rangle\langle Z_i| + |Z_i\rangle\langle N|$. The third term in eq 2 accounts for the coupling between electronic and vibrational degrees of freedom, while the last term describes the two harmonic oscillators associated with coordinates q_1 and q_2, with p_1 and p_2 representing the conjugated momenta.

Before addressing polar solvation, we must define the molecular dipole moment. For bent molecules, like **1**, two components of the molecular dipole moment operator must be introduced

$$\hat{\mu}_x = \mu_0 \sin\frac{\alpha}{2}(\hat{\rho}_1 - \hat{\rho}_2)$$
$$\hat{\mu}_y = \mu_0 \cos\frac{\alpha}{2}(\hat{\rho}_1 + \hat{\rho}_2) \quad (3)$$

where, μ_0 is the magnitude of the dipole moment relevant to either $|Z_1\rangle$ or $|Z_2\rangle$ and α is the angle between the two molecular arms. The x and y axes are aligned with the long and short molecular axis, respectively, with only x being relevant for linear molecules (like **2**) with $\alpha = 180°$.

As discussed in ref 32, sizable normal solvatochromism can be expected in bent quadrupolar chromophores. However the solvatochromism of **2**, a linear molecule, cannot be explained on this basis. On the other hand, attempts to describe the solvatochromism of **1** based on the bent molecule model and accounting for a single reaction field failed. In fact, to recover the observed solvatochromism, unphysically large deviations from linearity should be imposed, leading to a largely overestimated intensity of the secondary absorption band (cf. Supporting Information Figure S1). Therefore, here we introduce two independent reaction fields coupled with the charge distribution on each molecular arm. The total Hamiltonian, including solvation, reads

$$H = H_M - F_1\mu_0\hat{\rho}_1 - F_2\mu_0\hat{\rho}_2 + \frac{\mu_0^2F_1^2}{4\varepsilon_{or}} + \frac{\mu_0^2F_2^2}{4\varepsilon_{or}} \quad (4)$$

where F_1 and F_2 are the two reaction fields and ε_{or} measures the solvent relaxation energy.

Vibrational motion is treated exactly, in a truly nonadiabatic approach, while the reaction fields enter the problem as classical variables.[28,41,42] The Hamiltonian in eq 4 defines, for fixed F_1 and F_2 values, a coupled electron-vibration problem. The relevant Hamiltonian matrix is written on the basis defined as the direct product of the three electronic basis states times the eigenstates of the two harmonic oscillators associated with q_1

dx.doi.org/10.1021/jp3005508 | J. Phys. Chem. B 2012, 116, 4959−4966

and q_2. The two vibrational basis are truncated to the lowest M states, leading to a $3M^2 \times 3M^2$ matrix that is numerically diagonalized to get (numerically) exact results, provided that M is large enough to ensure convergence ($M = 8$ was used in this work). The resulting F_1 and F_2-dependent energies and eigenstates are used to calculate linear absorption and fluorescence spectra, as well as two-photon absorption and hyper-Rayleigh scattering spectra, according to explicit expressions given in refs 20, 41, and 42. The calculations are repeated on a grid of F_1 and F_2 values. Total spectra are finally obtained by summing up contributions from all points in the grid, weighted by the Boltzmann population on the relevant potential energy surface. Specifically, for one- and two-photon absorption and for hyper-Rayleigh scattering spectra, the Boltzmann population accounts for the (F_1,F_2)-dependent ground-state energy, while for emission spectra, the Boltzmann population of the fluorescent state is accounted for.

Figure 3 shows calculated spectra, to be compared with experimental spectra in Figure 1. Relevant model parameters

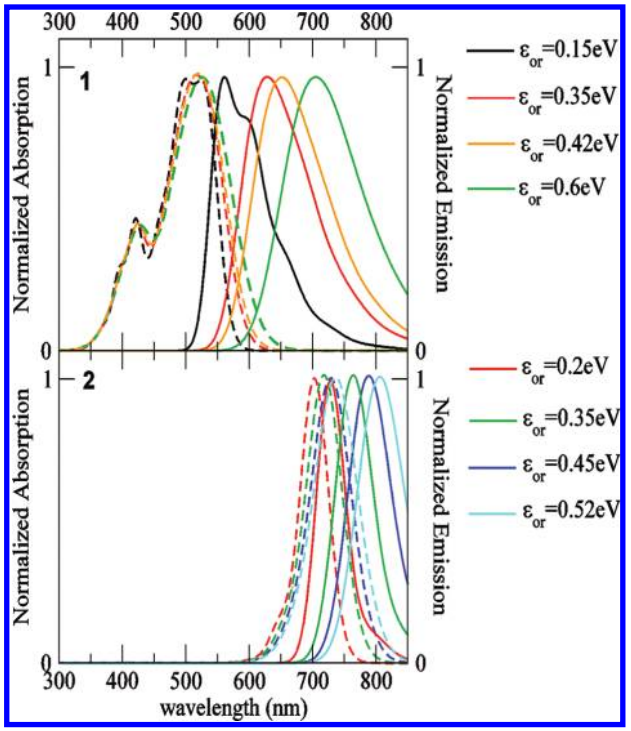

Figure 3. Calculated absorption and emission spectra of **1** (top panel) and **2** (bottom panel) in solvents of different polarity. Essential-state parameters are listed in Table 2.

are listed in Table 2. The agreement between experimental and calculated data is very good; accounting for two independent solvation fields, we quantitatively reproduce absorption and fluorescence solvatochromism as well as the band shape evolution with solvent polarity. For molecule **1**, the calculated intensity of the secondary peak is somewhat lower compared to experimental data, and the solvatochromic shifts are slightly underestimated. These effects can be ascribed to the presence of slightly solvatochromic bands, assigned to electronic transitions localized on either the electron-donor or electron-acceptor groups and partly overlapping the secondary peak. This hypothesis is confirmed by absorption spectra collected for two molecules mimicking the donor and acceptor groups, as described in the Supporting Information (Figure S4).

Table 2. Essential-State Parameters Adopted To Calculate Optical Spectra Reported in Figure 2[a]

	1	2
η (eV)	1.1	0.34
$(2)^{1/2}t$ (eV)	0.75	1.05
μ_0 (D)	28.6	19.2
α	120°	180°
ω_v(eV)	0.17	0.14
ε_v(eV)	0.45	0.12
γ (eV)	0.07	0.04

[a]The value of μ_0 only enters the definition of the molar extinction coefficient and is set to reproduce the experimental value in Table 1. The last parameter, γ, measures the intrinsic bandwidth of vibronic absorptions (cf. refs 41 and 42).

The same model, with exactly the same parameters, is adopted to calculate excitation anisotropy spectra following the procedure described in refs 37 and 43. Calculated anisotropy spectra of **2** are not shown because for this linear molecule, we calculate $r = 0.4$, in good agreement with experimental data in the lower panel of Figure 2. For **1**, the comparison between calculated anisotropy spectra in Figure 4 and experimental data

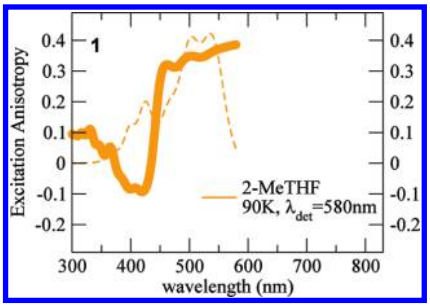

Figure 4. Calculated fluorescence excitation anisotropy spectra of **1**. Model parameters are listed in Table 2.

in the upper panel of Figure 2 is very satisfactory, particularly in the region from 450 to 580 nm, corresponding to the main absorption band. In the region of the secondary absorption band (~400 nm), the calculated anisotropy shows an abrupt decrease, approaching the theoretical lower limit $r \approx -0.2$. Experimental data show a less pronounced decrease in this region, a discrepancy ascribed to the partial overlap of the relevant band with other transitions located at higher energies, as confirmed by the absorption spectra (see the discussion above and Figure S4 in the Supporting Information).

Essential-state models, parametrized against linear absorption spectra, offer a computationally affordable approach for the calculation of nonlinear optical spectra and proved very successful in several instances.[28,31,41−48] Figures 5 and 6 show HRS and TPA spectra calculated for **1** and **2** with model parameters in Table 2 for two ε_{or} values to mimic low- and high-polarity solvents. For the bent molecule, **1**, the two electronic excited states responsible for the main (g → c) and secondary (g → e) absorption bands are expected to give sizable contributions to the HRS and TPA signals. Calculated spectra in Figure 5 confirm this prediction. A weak TPA intensity is in fact observed in the region of the main (g → c) absorption peak that would be forbidden for linear symmetrical molecules. Most of the TPA intensity is however found in the region of the secondary (g → e) absorption, corresponding to the allowed TPA band for a linear molecule. Instead, the

dx.doi.org/10.1021/jp3005508 | J. Phys. Chem. B 2012, 116, 4959−4966

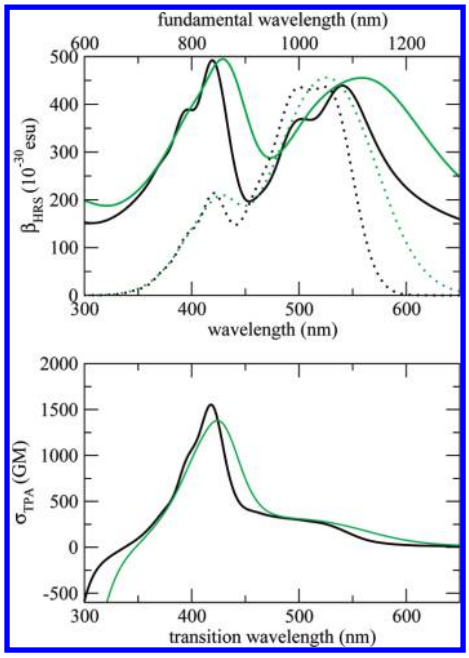

Figure 5. Calculated HRS (top panel) and TPA spectra (bottom panel) for **1**, adopting model parameters in Table 2 and setting ε_{or} = 0.15 (black lines) and 0.6 eV (green lines), corresponding to simulated spectra in cyclohexane and dichloromethane, respectively (cf., the top panel of Figure 3). Dotted lines in the upper panel show calculated linear absorption spectra in arbitrary units.

calculated HRS signal is large (of similar magnitude as that calculated for an octupolar chromophore[42]), in correspondence with both the main and secondary bands. Solvent polarity has

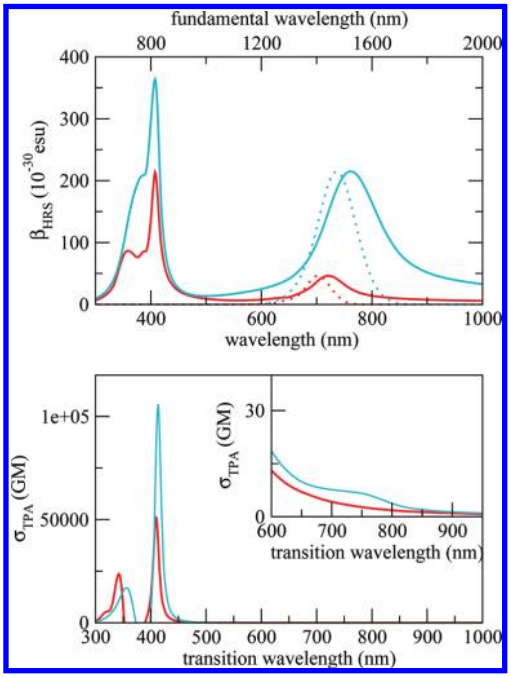

Figure 6. Calculated HRS (top panel) and TPA spectra (bottom panel) for **2**, adopting model parameters in Table 2 and setting ε_{or} = 0.20 (red lines) and 0.52 eV (cyan lines), corresponding to simulated spectra in toluene and glycerol, respectively (cf., the bottom panel of Figure 3). Dotted lines in the upper panel show calculated linear absorption spectra in arbitrary units.

minor effects in both HRS and TPA spectra of **1**. HRS peaks indeed broaden in polar solvents, leading to a large HRS response in a wide spectral region, with $\beta_{HRS} > 300 \times 10^{-30}$esu in the 700−1300 nm interval for simulated spectra in dichloromethane. Inhomogeneous broadening effects are also recognized in the red shift of HRS features with respect to the OPA peak.[42]

TPA spectra of **2** are largely dominated by the very intense feature typical of squaraine dyes, associated with the highest-energy (g → e) transition, almost resonant with the linear absorption peak.[28] Due to the linear structure of **2**, the g → c transition is forbidden in TPA, and just a very weak shoulder is calculated in this spectral region in the TPA spectrum relevant to the most polar solvent. This weak feature is associated with the lowering of molecular symmetry in polar solvents. In fact, in the proposed model for polar solvation, the two reaction fields, F_1 and F_2, associated with the two molecular arms, are mutually independent and, when $F_1 \neq F_2$, the molecular symmetry is lowered, allowing for a (weak) TPA intensity of the nominally forbidden g → c transition. More interesting are HRS spectra; because the molecule is linear (and strictly so in our model), the calculated HRS intensity can only derive from symmetry lowering due to polar solvation, as also confirmed by the large dependence of the HRS intensity on ε_{or}. However, while symmetry lowering has minor effects on TPA spectra, its effects on HRS spectra are very important. Indeed, the HRS signal becomes, in the most polar solvent, as large as that for the bent molecule **1** or that for the octupolar chromophore in ref 42. Large inhomogeneous broadening effects in HRS spectra have already been discussed in terms of band shapes and band positions.[42,49] Here, we emphasize that starting from symmetrical structures, the symmetry lowering related to polar solvation can lead to sizable HRS intensities.

The different sensitivity of HRS and TPA spectra of linear quadrupolar molecules to symmetry-lowering perturbations can be rationalized based on simple perturbative arguments. Solvent-induced symmetry lowering is driven by $\Delta = F_1 - F_2$. A perturbative expansion on Δ of the electronic states relevant to the symmetric ($\Delta = 0$) structure, $|g\rangle$, $|c\rangle$, and $|e\rangle$ (see the discussion above and ref 28 for more details), leads to three Δ-dependent electronic eigenstates

$$|g(\Delta)\rangle = |g\rangle - \frac{\mu_{gc}}{\omega_{gc}}\Delta|c\rangle$$

$$|c(\Delta)\rangle = |c\rangle + \frac{\mu_{gc}}{\omega_{gc}}\Delta|g\rangle - \frac{\mu_{ce}}{\omega_{ce}}\Delta|e\rangle$$

$$|e(\Delta)\rangle = |e\rangle + \frac{\mu_{ce}}{\omega_{ce}}\Delta|c\rangle$$

where $\mu_{gc} = \langle c|\mu|g\rangle$ and $\mu_{ge} = \langle e|\mu|g\rangle$ are the transition dipole moments of the g → c and g → e transitions of the symmetric system and ω_{gc} and ω_{ce} are the corresponding transition frequencies. Inserting these expressions into standard equations for HRS and TPA signals, one easily recognizes that perturbative corrections to the HRS signal grow linearly with Δ, while the leading term in the TPA intensity of the g → c transition is proportional to Δ^2, then representing a minor correction. We emphasize that symmetry-lowering effects in HRS spectra are particularly important because of the presence of two independent reaction fields in the model that largely increase the density of asymmetric states.

dx.doi.org/10.1021/jp3005508 | J. Phys. Chem. B 2012, 116, 4959−4966

5. DISCUSSION AND CONCLUSION

The broad absorption and emission spectra of **1** contrast with the narrow spectral features of **2**. Narrow spectral features are, in general, characteristic of squaraine dyes and are related to the relatively small electron-vibration coupling in these systems (small ε_v) and to the large mixing between the neutral and zwitterionic states, typical of class II quadrupolar dyes,[28] that further reduces the effective vibrational coupling. Broad absorption and fluorescence bands of **1** are instead typical of largely neutral (class I) chromophores.[28] These features hold true also in the model discussed in this paper, accounting for two independent reaction fields. The main spectroscopic consequence of the presence of two reaction fields is recognized in the sizable normal solvatochromism of linear absorption spectra that cannot be rationalized in models accounting for a single reaction field.

Essential-state models for nonlinear V-shaped quadrupolar chromophores, like **1**, have been recently discussed.[32] The appearance of a secondary band in the linear absorption spectra, to the blue of the main band, marks the reduced symmetry of bent molecules; the g → e transition, OPA-forbidden and TPA-allowed in linear molecules, acquires a sizable OPA intensity in bent molecules. This makes the overall absorption spectrum of V-shaped quadrupolar chromophores very broad; **1**, a largely neutral chromophore, showing in the green spectral region the typical broad absorption band of class I dyes, shows an additional peak in the blue−violet region, due to its V-shaped structure. The resulting absorption spectrum then covers most of the solar spectrum, making this chromophore, and more generally V-shaped quadrupolar chromophores, promising for solar cell applications.

Both **1** and **2** show an anomalous red shift of the absorption band upon increasing solvent polarity. In line with the bulky nature of substituent groups, we explain this observation, accounting for two independent reaction fields associated with the two molecular arms. The resulting model quantitatively reproduces experimental absorption and fluorescence spectra and their dependence on the solvent polarity, based on a small number of adjustable model parameters. The model is then used to calculate nonlinear optical spectra of the two chromophores. As expected, the bent structure of **1** shows up with sizable TPA intensity related to both g → c and g → e transitions and with a fairly large HRS intensity. More intriguing is the behavior of **2**; in line with its linear structure, TPA spectra of **2** are largely dominated by the g → e transition, as expected on symmetry grounds. However, an intense HRS spectrum is calculated for **2**, a linear and nominally symmetric molecule. This anomalous intensity is ascribed to symmetry lowering in polar solvents that, in the present system, are largely amplified by the presence of two independent reaction fields.

In this paper, we highlight that the presence of bulky substituent groups strongly influences the spectroscopic properties of quadrupolar molecules, giving rise to unexpected effects related to symmetry breaking. Bulky terminal groups may break down the coherence between the two arms of the molecule, so that each arm responds to a different reaction field in polar solvents, leading to sizable solvatochromism in both absorption and fluorescence spectra. The presence of two independent reaction fields amplifies inhomogeneous broadening effects with particularly impressive effects on nonlinear optical spectra.

■ ASSOCIATED CONTENT

Ⓢ Supporting Information

Figures S1−S3 show spectra calculated for the two compounds with slightly different models. Figure S4 shows experimental absorption spectra of chemical species mimicking the isolated electron-acceptor and electron-donor groups. This material is available free of charge via the Internet at http://pubs.acs.org.

■ AUTHOR INFORMATION

Corresponding Author

*E-mail: anna.painelli@unipr.it. Tel. +39 0521 905461. Fax +39 0521 905556.

Notes

The authors declare no competing financial interest.

■ ACKNOWLEDGMENTS

This work was partly supported by the Indo−Italian Executive Programme of Scientific and Technological Co-operation 2008−2010 and by Fondazione Cariparma through the Project 2010.0329. C.S. thanks the University of Parma and INSTM for financial support. S.P. thanks the ISRO-IISc Space Technology Cell for supporting this work through the Project ISTC/CSS/STP/252, and S.R.B.K. thanks CSIR for a Senior Research Fellowship.

■ REFERENCES

(1) Reichardt, C. *Chem. Rev.* **1994**, *94*, 2319−2358.
(2) Le Droumaguet, C.; Mongin, O.; Werts, M. H. V.; Blanchard-Desce, M. *Chem. Commun.* **2005**, 2802−2804.
(3) Fromherz, P.; Hubener, G.; Kuhn, B.; Hinner, M. J. *Eur. Biophys. J.* **2008**, *37*, 509−514.
(4) Reichardt, C. *Pure Appl. Chem.* **2008**, *80*, 1415−1432.
(5) Signore, G.; Nifos, R.; Albertazzi, L.; Storti, B.; Bizzarri, R. *J. Am. Chem. Soc.* **2010**, *132*, 1276−1288.
(6) Marcus, R. A. *Rev. Mod. Phys.* **1993**, *65*, 599−610.
(7) Kanis, D. R.; Ratner, M. A.; Marks, T. J. *Chem. Rev.* **1994**, *94*, 195−242 and references therein..
(8) Brédas, J.-L.; Cornil, K.; Meyers, F.; Beljonne, D. In *Handbook of Conducting Polymers*; Skotheim, T. A., Elsenbaumer, R. L., Reynolds, J. R., Eds; Marcel Dekker: New York, 1998; pp 1−26.
(9) Pati, S. K.; Marks, T. J.; Ratner, M. A. *J. Am. Chem. Soc.* **2001**, *123*, 7287−7291.
(10) (a) Datta, A.; Pati, S. K. *J. Phys. Chem. A* **2004**, *108*, 9527−9530. (b) Datta, A.; Pati, S. K. *J. Phys. Chem. A* **2004**, *108*, 320−325. (c) Datta, A.; Pati, S. K. *J. Chem. Phys.* **2003**, *118*, 8420−8427.
(11) Dalton, L. R.; Sullivan, P. A.; Bale, D. H. *Chem. Rev.* **2010**, *110*, 25−55.
(12) Perez-Moreno, J.; Zhao, Y.; Clays, K.; Kuzyk, M. G.; Shen, Y.; Qiu, L.; Hao, J.; Guo, K. *J. Am. Chem. Soc.* **2009**, *131*, 5084−5093.
(13) Metzger, R. M. *Chem. Rev.* **2003**, *103*, 3803−3834.
(14) Martin, S.; Sambles, J. R.; Ashwell, G. J. *Phys. Rev. Lett.* **1993**, *70*, 218−221.
(15) Terenziani, F.; Painelli, A.; Girlando, A.; Metzger, R. M. *J. Phys. Chem. B* **2004**, *108*, 10743−10750.
(16) Girlando, A.; Sissa, C.; Terenziani, F.; Painelli, A.; Chwialkowska, A.; Ashwell, G. J. *ChemPhysChem* **2007**, *8*, 2195−2201.
(17) Tan, O.; Clark, S. J.; Szablewski, M.; Cross, G. H. *J. Chem. Phys.* **2010**, *133*, 244702−244708.
(18) Beljonne, D.; Wenseleers, W.; Zojer, E.; Shuai, Z. G.; Vogel, H.; Pond, S. J. K.; Perry, J. W.; Marder, S. R.; Bredas, J. L. *Adv. Funct. Mater.* **2002**, *12*, 631−641.
(19) Mongin, O.; Porrés, L.; Charlot, M.; Katan, C.; Blanchard-Desce, M. *Chem.—Eur. J.* **2007**, *13*, 1481−1498.
(20) Terenziani, F.; Katan, C.; Badaeva, E.; Tretiak, S.; Blanchard-Desce, M. *Adv. Mater.* **2008**, *20*, 4641−4678.

(21) Beverina, L.; Crippa, M.; Landenna, M.; Ruffo, R.; Salice, P.; Silvestri, F.; Versari, S.; Villa, A.; Ciaffoni, L.; Collini, E.; et al. *J. Am. Chem. Soc.* **2008**, *130*, 1894−1902.
(22) Pawlicki, M.; Collins, H. A.; Denning, R. G.; Anderson, H. L. *Angew. Chem., Int. Ed.* **2009**, *48*, 3244−3266.
(23) Ramaiah, D.; Joy, A.; Chandrasekhar, N.; Eldho, N. V.; Das, S.; George, M. V. *Photochem. Photobiol.* **1997**, *65*, 783−790.
(24) Salice, P.; Arnbjerg, J.; Pedersen, B. W.; Toftegaard, R.; Beverina, L.; Pagani, G. A.; Ogilby, P. R. *J. Phys. Chem. A* **2010**, *114*, 2518−2525.
(25) Do, J.; Huh, J.; Kim, E. *Langmuir* **2009**, *25*, 9405−9412.
(26) Painelli, A.; Terenziani, F. *ChemPhysChem* **2009**, *10*, 527−531.
(27) (a) Alex, S.; Santhosh, U.; Das, S. *J. Photochem. Photobiol. A* **2005**, *172*, 63−71. (b) Yum, J.-H.; Walter, P.; Huber, S.; Rentsch, D.; Geiger, T.; Nüesch, F.; De Angelis, F.; Grätzel, M.; Nazeeruddin, M. K. *J. Am. Chem. Soc.* **2007**, *129*, 10320−10321. (c) Silvestri, F.; Irwin, M. D.; Beverina, L.; Facchetti, A.; Pagani, G. A.; Marks, T. J. *J. Am. Chem. Soc.* **2008**, *130*, 17640−17641. (d) Xue, L.; He, J.; Gu, X.; Yang, Z.; Xu, B.; Tian, W. *J. Phys. Chem. C* **2009**, *113*, 12911−12917.
(28) Terenziani, F.; Painelli, A.; Katan, C.; Charlot, M.; Blanchard-Desce, M. *J. Am. Chem. Soc.* **2006**, *128*, 15742−15755.
(29) Strehmel, B.; Sarker, A. M.; Detert, H. *ChemPhysChem* **2003**, *4*, 249−259.
(30) (a) Rouxel, C.; Charlot, M.; Mir, Y.; Frochot, C.; Mongin, O.; Blanchard-Desce, M. *New J. Chem.* **2011**, *35*, 1771−1780. (b) Panthi, K.; Adhikari, R. M.; Kinstle, T. H. *J. Phys. Chem. A* **2010**, *114*, 4542−4549.
(31) Terenziani, F.; Przhonska, O. V.; Webster, S.; Padilha, L. A.; Slominsky, Y. L.; Davydenko, I. G.; Gerasov, A. O.; Kovtun, Y. P.; Shandura, M. P.; Kachkovski, A. D; et al. *J. Phys. Chem. Lett.* **2010**, *1*, 1800−1804.
(32) Ponterini, G.; Vanossi, D.; Krasnaya, Z. A.; Tatikolovc, A. S.; Momicchioli, F. *Phys. Chem. Chem. Phys.* **2011**, *13*, 9507−9517.
(33) Wojcik, A.; Nicolaescu, R.; Kamat, P. V.; Chandrasekaran, Y.; Patil, S. *J. Phys. Chem. A* **2010**, *114*, 2744−2750.
(34) Mukhopadhyay, S.; Kanth, S. R. B.; Ramasesha, S.; Patil, S. *J. Phys. Chem. A* **2010**, *114*, 4647−4654.
(35) Chou, S. P.; Yu, C. *Synth. Met.* **2004**, *142*, 259−262.
(36) Chandrasekharan, Y.; Dutta, G. K.; Kanth, S. R. B.; Patil, S. *Dyes Pigm.* **2009**, *83*, 162−167.
(37) Sissa, C.; Painelli, A.; Blanchard-Desce, M.; Terenziani, F. *J. Phys. Chem. B* **2011**, *115*, 7009−7020.
(38) Terenziani, F.; Painelli, A. *Chem. Phys.* **2003**, *295*, 35−46.
(39) Lakowicz, J. R. *Principles of Fluorescence Spectroscopy*; Kluwer Academic/Plenum Publishers: New York, 1999.
(40) Webster, S.; Fu, J.; Padilha, L. A.; Przhonska, O. V.; Hagan, D. J.; Van Stryland, E. W.; Bondar, M. V.; Slominsky, Y. L.; Kachkovski, A. D. *Chem. Phys.* **2008**, *348*, 143−151.
(41) Grisanti, L.; Sissa, C.; Terenziani, F.; Painelli, A.; Roberto, D.; Tessore, F.; Ugo, R.; Quici, S.; Fortunati, I.; Garbin, E; et al. *Phys. Chem. Chem. Phys.* **2009**, *11*, 9450−9457.
(42) Campo, J.; Painelli, A.; Terenziani, F.; Van Regemorter, T.; Beljonne, D.; Goovaerts, E.; Wenseleers, W. *J. Am. Chem. Soc.* **2010**, *132*, 16467−16478.
(43) Grisanti, L.; Terenziani, F.; Sissa, C.; Cavazzini, M.; Rizzo, F.; Orlandi, S.; Painelli, A. J. *Phys. Chem. B* **2011**, *115*, 11420−11430.
(44) Terenziani, F.; Sissa, C.; Painelli, A. *J. Phys. Chem. B* **2008**, *112*, 5079−5087.
(45) Sissa, C.; Terenziani, F.; Painelli, A.; Abbotto, A.; Bellotto, L.; Marinzi, C.; Garbin, E.; Ferrante, C.; Bozio, R. *J. Phys. Chem. B* **2010**, *114*, 882−893.
(46) Todescato, F.; Fortunati, I.; Carlotto, S.; Ferrante, C.; Grisanti, L.; Sissa, C.; Painelli, A.; Colombo, A.; Dragonetti, C.; Roberto, D. *Phys. Chem. Chem. Phys.* **2011**, *13*, 11099−11109.
(47) Sissa, C.; Parthasarathy, V.; Drouin-Kucma, D.; Werts, M. H. V.; Blanchard-Desce, M.; Terenziani, F. *Phys. Chem. Chem. Phys.* **2010**, *12*, 11715−11727.
(48) (a) Terenziani, F.; Parthasarathy, V.; Pla-Quintana, A.; Maishal, T.; Caminade, A.-M.; Majoral, J.-P.; Blanchard-Desce, M. *Angew. Chem., Int. Ed.* **2009**, *48*, 8691−8694. (b) Terenziani, F.; Ghosh, S.; Robin, A.-C.; Das, P. K.; Blanchard-Desce, M. *J. Phys. Chem. B* **2008**, *112*, 11498−11505.
(49) Campo, J.; Wenseleers, W.; Goovaerts, E.; Szablewski, M.; Cross, G. *J. Phys. Chem. C* **2008**, *112*, 287−296.